Available online at www.sciencedirect.com

ScienceDirect

Journal of Photochemistry and Photobiology A: Chemistry 195 (2008) 337–345

Journal of Photochemistry and Photobiology A:Chemistry

www.elsevier.com/locate/jphotochem

New polyacrylates with photosensitive triazene groups designed for laser ablation Synthesis, structure and properties

Emil C. Buruiana [a,*], Lenuta Hahui [a], Tinca Buruiana [a], Lukas Urech [b], Thomas Lippert [b]

[a] Petru Poni Institute of Macromolecular Chemistry, 41 A Gr. Ghica Voda Alley, 700487 Iasi, Romania

[b] Paul Scherrer Institute, 5232 Villigen PSI, Switzerland

Received 18 July 2007; received in revised form 25 October 2007; accepted 29 October 2007

Available online 4 November 2007

Abstract

Two new triazene monomers, such as (1-(*para* methoxy-phenyl)-3-(2 acryloyloxyethyl)-3-methyl triazene-1, M_1) and (1-(*para* chloro-phenyl)-3-(2 acryloyloxyethyl)-3-methyl triazene-1, M_2) were synthesized and further employed as reaction partners with methyl methacrylate (MMA) in order to investigate the substituent effect of the triazene moiety on the polymeric properties. The synthesized monomers and polymers (PA1, molar fraction of $M_1 = 0.16$; PA2, molar fraction of $M_2 = 0.11$) were characterized by analytical and spectroscopic methods, while the surface morphology of polymers was visualized by atomic force microscopy (AFM) and optical microscopy. The photosensitivity of these copolymers was evaluated upon UV exposure, in solution and in film state, following the decreasing value of the π–π^* absorption band corresponding to the triazene group centered at 290 nm and 320 nm. For both copolymers, the kinetic data indicated a first-order photoprocess, as evidenced from the determined constant rate in film state (PA1, $k = 2.3 \times 10^{-3}\ s^{-1}$; PA2, $k = 2.7 \times 10^{-4}\ s^{-1}$). Moreover, the ablation characteristics achieved at low fluence for an irradiation wavelength of 308 nm, quality structuring with no any debris and the absence of carbonization of the irradiated areas suggest that such photolabile polyacrylates could offer new possibilities in printing techniques and nanostructures on surfaces. In addition, the triazene functions introduced as side groups may be used for the tailoring of special polymeric architectures.

© 2007 Elsevier B.V. All rights reserved.

Keywords: Photosensitive; Triazene; Polyacrylates; UV/laser ablation; Copolymers

1. Introduction

In recent years, the design of photosensible polymeric architectures occupies a central place in the development of functional devices for specialized applications like photoresponsive systems [1], medical applications [2] and optical data storage [3]. Among them, the photolabile polymers have been of increasing interest because of their importance in the modern communication techniques or for nanotechnology applications, impossibly to imagine without such new polymeric materials which can be structured by light or, more recently, by lasers [4]. For example, a series of triazene polymers tailored for laser-induced polymer processing, ranging from surface modification, ablative photodecomposition to thin film deposition have been intensively investigated [5] to be exploited in microlithography [1] and photoresist technique [6] owing to the intrinsic qualities of photo removable triazene chromophore. Generally, the dominating aspects that can succeed the performance of photoresist systems are the dimensions, resolution and sensitivity of systems during the irradiation process. As a result of the observed process, the promising candidates to accomplish these particular conditions are those that can be structured by the dry development of structuring techniques [7] such as excimer laser lithography. Such “dry etching” capability has the advantage that no additional wet-developing steps are necessary after irradiation, making this technique attractive for industrial applications (the manufacturing of film transistors—liquid crystals displays) [8].

In relation to polymers intended for photolithographic processes, the literature studies were focused primarily on microstructuring of standard polymers (polyimides, polymethacrylates, polycarbonates, polyester, etc.) [9,10] or on doped systems (polymers/rodhamine, pyrene, benzophenone, etc.) [11] through UV/laser irradiation, but often, the quality of the ablated zones is relatively poor, with ablation debris con-

* Corresponding author.
E-mail address: emilbur@icmpp.ro (E.C. Buruiana).

1010-6030/$ – see front matter © 2007 Elsevier B.V. All rights reserved.
doi:10.1016/j.jphotochem.2007.10.021

taminating the surfaces. Given the above points, several authors suggested that the triazene polymers can be developed for laser ablation using 308 nm irradiation because the triazene group (–N=N–N<) is able to undergo a photochemical decomposition with the release of molecular nitrogen acting as driven and carriers gases of ablation [12].

In contrast, it was established that the ablation properties are not satisfactory in the case of polymers containing triazene derivatives physically incorporated in the matrix (over 10 wt.% loading) owing to an agglomeration of the dopant, which may cause inhomogeneous ablation [13]. One approach to solving this problem is to employ polymers with triazene moiety covalently attached to the backbone and from this reason it is of interest in the design and synthesis of new triazene polymers with improved properties that could be used as <true> dry etching resists with no additional cleaning steps. In most cases, these photopolymers revealed superior ablation, i.e. low ablation threshold, high ablation rates and high quality structuring without debris [14,15]. Another advantage of the triazene polymers is the absence of carbonization of the irradiated areas which is very pronounced for polymers with similar absorption coefficients at 308 nm, such as Kapton [16]. Recently, novel polymers based on the triazene function and new UV-laser applications of them have been developed, i.e. as sacrificial dynamic release layer in laser-induced forward transfer processes [17–19]. For this purpose, it is very important that the polymers chosen to have good film-forming properties in a range of solvents and different surface properties.

As a continuation of our effort to accomplish a better understanding of the effect of the triazene chromophore on the polymer properties [20,21], in this paper we report the synthesis and characterization of triazene polyacrylates as a new class of functional materials with promising potential for processes following the laser structuring compared to the UV-light, temperature and other acid sensitive triazene polymers, where a flexible production of small number is the goal. Taking advantage of the dependence between nature and structure of the triazene monomers and macroscopic properties of the resulting polymers, we demonstrate that the change of the substituent attached to the triazene chromophore from the polyacrylate backbone is a structural variable that control the photosensitivity and the laser ablation characteristics of polymers.

2. Experimental

2.1. Synthetic procedure

Two different acrylic monomers with triazene moieties were synthesized in a two steps procedure, as shown in Scheme 1.

2.1.1. Intermediates synthesis

I_1: 1-(*para* methoxy-phenyl)-3-(2 hydroxyethyl)-3-methyl triazene-1 was prepared according to the methods described in the literature [20]. Thus, *p*-anisidine (5 g, 40.6 mmol) is dissolved in 26.44 mL of 12% hydrochloric acid. Sodium nitrite (2.8 g, 40.6 mmol) in 40 mL water is added slowly at 0 °C and the mixture was kept under stirring for 30 min. The resulting solution of diazonium salt is transferred into a cooled addition funnel and it is slowly dropped into a mixture of 3 g *N*-methyl ethanolamine (40.6 mmol) and 16.8 g (101.5 mmol) of sodium carbonate in 50 mL water at 0–5 °C, maintaining the pH above 7. Then, the mixture is stirred for another 30 min, while 5 g of NaCl is added and the temperature is raised to 20 °C. Next, the

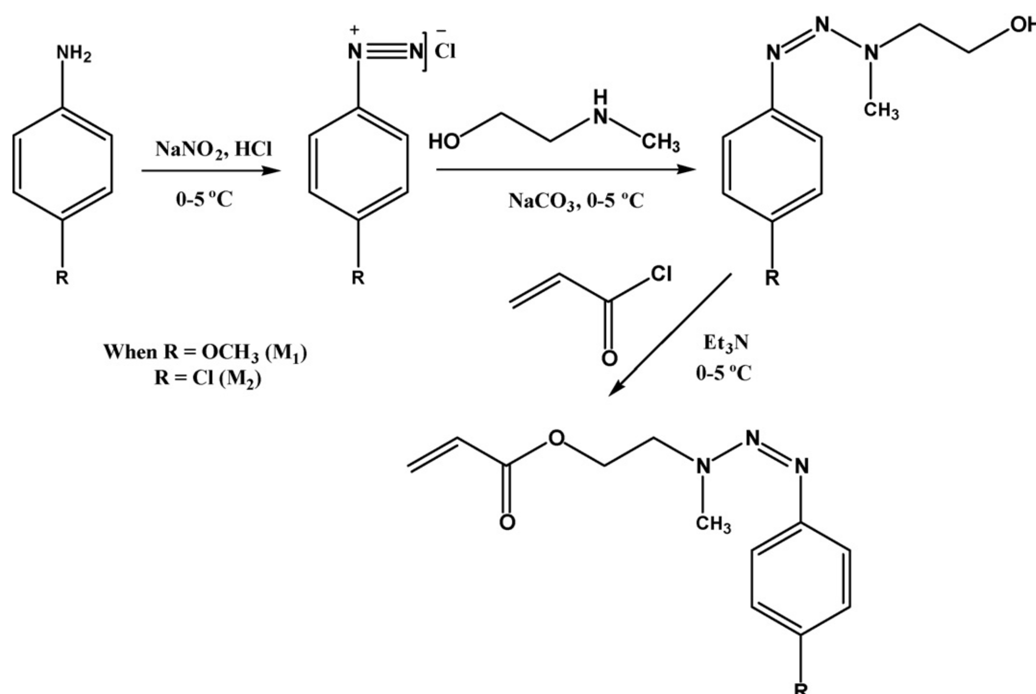

Scheme 1. Synthesis of triazene monomers M_1 and M_2.

mixture was extracted two times with Et_2O, dried on Na_2SO_4 and concentrated under vacuum, when brown viscous oil is collected. Yield ($C_{10}H_{15}O_2N_3$): 6.3 g, 79%, Elem. Anal. Calcd.: C, 57.4%; H, 7.23%; N, 20.08%. Found: C, 57.3%; H, 7.2%; N, 20.0%.

I_2: 1-(*para* chloro-phenyl)-3-(2 hydroxyethyl)-3-methyl triazene-1 was prepared using the same procedure described above. Yield ($C_9H_{12}N_3OCl$): 11.5 g, 73%, Elem. Anal. Calcd.: C, 50.59%; H, 5.66%; N, 19.67%; Cl, 16.59%. Found: C, 50.56%; H, 5.62%; N, 19.63%; Cl, 16.53%.

2.1.2. Monomer synthesis

M_1: The above intermediate I_1 (4.3 g, 20 mmol) was dissolved in methylene chloride and the solution was cooled in an ice/salt/water bath. After, 1.66 mL (20 mmol) of acryloyl chloride was added drop wise with vigorous stirring in the presence of triethyl amine (3.33 mL, 20 mmol). This mixture was maintained at room temperature under stirring for three days, filtered, extracted, washed several times with water and than dried over Na_2SO_4. After removing of solvent, a triazene acrylic monomer (1-(*para* methoxy-phenyl)-3-(2 acryloyloxyethyl)-3-methyl triazene-1) was collected (M_1). Yield ($C_{13}H_{17}N_3O_3$): 4.5 g, 73%, Elem. Anal. Calcd.: C, 59.3%; H, 6.51%; N, 15.96%. Found: C, 59.24%; H, 6.48%; N, 15.9%.

M_2: Similar treatment was performed for I_2 in order to obtain 1-(*para* chloro-phenyl)-3-(2 acryloyloxyethyl)-3-methyl triazene-1 as the second monomer (M_2). Yield ($C_{12}H_{14}N_3O_2Cl$): 14.2 g, 90%, Elem. Anal. Calcd.: C, 53.84%; H, 5.27%; N, 15.7%; Cl, 13.2%. Found: C, 53.8%; H, 5.25%; N, 15.64%; Cl, 13.1%.

2.1.3. Polymer synthesis

The general structure of triazene polyacrylates: 1-(*para* methoxy-phenyl)-3-(2 acryloyloxyethyl)-3-methyl triazene-1-co-methyl methacrylate (PA1) and 1-(*para* chloro-phenyl)-3-(2 acryloyloxyethyl)-3-methyl triazene-1-co-methyl methacrylate (PA2) employed in our study can be revealed in Scheme 2. For the preparation of acrylic copolymers (PA1 and PA2), monomers M_1 or M_2 and methylmethacrylate (MMA) were dissolved in dioxane (30 wt.%) into a molar ratio of 1:2.33 using 0.2% AIBN as initiator. The reaction mixture was flushed with argon and placed in oven at 60 °C. After 3 days the reaction was finished and the polymer precipitated in a large amount of methanol and dried for 48 h under reduced pressure.

PA1: Yield 79%, Elem. Anal. Calcd.: C, 59.79%; H, 7.53%; N, 4.86%. Found: C, 59.72%; H, 7.45%; N, 4.8%.

PA2: Yield 73%, Elem. Anal. Calcd.: C, 58.48%; H, 7.31%; N, 4.49%; Cl, 3.32%. Found: C, 58.4%; H, 7.28%; N, 4.42%; Cl, 3.29%.

2.2. Measurements

I_1: ^1H NMR ($CDCl_3$, δ ppm): 7.34 (d, 2H, aromatic protons in *ortho* position to triazene groups), 6.83 (d, 2H, aromatic protons in *meta* position to triazene groups), 3.77 (t, 4H, CH_2CH_2OH), 3.73 (s, 3H, OCH_3), 3.21 (s, 3H, CH_3–N–N=N), 2.77 (d, 1H, OH); FTIR (KBr, cm^{-1}): 3400 (OH), 2900 (CH), 1595 (aromatic ring), 1350 (N=N–N), 1190 (OCH_3), 850 (disubstituted aromatic ring).

I_2: ^1H NMR (DMSO-d_6, δ ppm): 7.43 (s, 4H, aromatic protons), 4.9 (s, 1H, OH), 3.83 (t, 2H, CH_2CH_2OH), 3.71 (m, 2H, CH_2CH_2OH), 3.20 (s, 3H, CH_3–N–N=N); FTIR (KBr, cm^{-1}): 3350 (OH), 2920 (CH), 1550 (aromatic ring), 1350 (N=N–N), 850 (disubstituted aromatic ring).

M_1: ^1H NMR (DMSO-d_6, δ ppm): 7.2 (d, 2H, aromatic protons in *ortho* position to triazene groups), 6.83 (t, 2H, *meta* aromatic protons to triazene), 6.2 (d, 1H, *trans* olefinic proton CH_2), 6.1 (m, 1H, olefinic proton CH), 5,78 (m, 1H, *cis* olefinic proton CH_2) 4,35 (t, 2H, CH_2CH_2OCO), 4.0 (t, 2H, CH_2CH_2OCO); 3.70 (s, 3H, OCH_3), 3.3 (s, 3H, CH_3–N–N=N), FTIR (KBr, cm^{-1}): 1750 (C=O), 1625 (C=C), 1595 (aromatic CH), 1300 (N=N–N), 1190 (OCH_3), 850 (disubstituted aromatic ring).

M_2: ^1H NMR (DMSO-d_6, δ ppm): 7.42 (s, 4H, aromatic protons), 6.15 (d, 1H, *trans* olefinic proton), 6.13 (m, 1H, olefinic proton), 5.8 (d, 1H, *cis* olefinic proton), 4.4 (t, 2H, CH_2CH_2OCO), 4.05 (m, 2H, CH_2CH_2OCO), 3.20 (s, 3H, CH_3–N–N=N); FTIR (KBr, cm^{-1}): 1726 (C=O), 1635 (C=C), 1599 (aromatic), 1352 (N=N–N), 834 (disubstituted aromatic ring).

PA1: ^1H NMR (DMSO-d_6, δ ppm): 7.30 (m, aromatic protons in *ortho* position to triazene group), 6.9 (m, aromatic protons in *meta* position to triazene group), 4.14–3.75 (CH_2–CH_2 from M_1), 3.70 (OCH_3) 3.54 (–$COOCH_3$ from MMA), 3.17

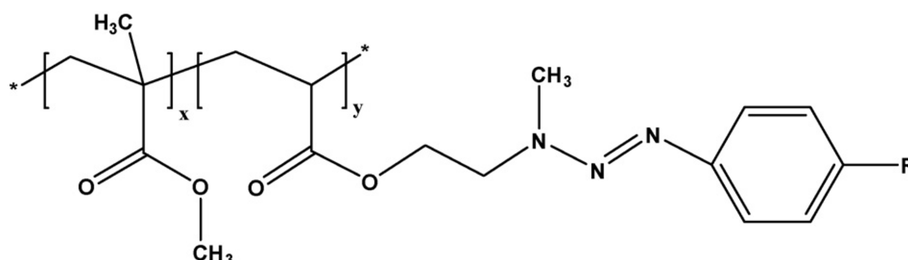

Scheme 2. The structure of triazene polyacrylates (PA1 and PA2).

($N–CH_3$), 2.1–1.4 (CH–COO–), 1.35–0.74 (CH_2 from M_1; CH_2 and CH_3 from MMA).
PA2: ^{1}H NMR (DMSO-d$_6$, δ ppm): 7.33 (t, aromatic protons), 4.42–4.0 ($CH_2–CH_2$ from M_2), 3.6 ($COOCH_3$ from MMA), 3.2 (CH_3–N), 2–1.4 (CHCOO–), 1.3–0.7 (CH_2 from M_2; CH_2 and CH_3 from MMA).

2.3. Equipment

The polymer structures were verified by ^{1}H NMR, FTIR and UV spectroscopy using a Bruker 400-MHz spectrometer with tetramethylsilane as an internal standard, a Bruker Vertex 70 and a Specord M42 spectrophotometer, respectively. Gel permeation chromatography (GPC) measurements were determined with a PL MD-950 instrument (Polymer Laboratories) equipped with an evaporative mass detector and two PL gel 5 μm columns. The thermal transitions were measured on a PerkinElmer differential scanning calorimeter by cooling of the polymer to −20 °C and heating at a rate of 10 °C min^{-1} up to 200 °C, while the thermal stability of the polyacrylates was analyzed through thermogravimetry using a MOM Budapest derivatograph. TGA thermograms were recorded between 20 °C and 600 °C with a heating rate of 12 °C min^{-1} in air. UV irradiations were performed in solution and in thin films, using a 500 W high-pressure mercury lamp without wavelength selection, at room temperature. A SOLVER PRO-M atomic force microscope was used to probe the surface morphology. The film thickness of the films was determined with an interferential microscope (Linnik). The laser ablation rate and the ablation threshold fluence (F_{th}) were obtained by the irradiation of solvent-cast polymer films with a XeCl laser (wavelength = 308 nm, pulse length (τ) = 30 ns; Compex 205, Lambda Physic), using a laser beam with a uniform flat profile. To cut a homogeneous part of the larger beam, a square mask of 5 mm × 5 mm and a spot size of 500 μm were utilized. The resulting ablation craters in the polymer were measured with a Sloan Dektak 8000 profilometer (Veeco) and were plotted against the pulse number for each irradiation fluence (F). The slopes of these individual curves corresponded to the ablation rates for the corresponding fluence. The ablation rates were then plotted versus the fluence and fitted according to Eq. (1) [22]:

$$d(F) = \frac{1}{\alpha_{eff}} \ln\left(\frac{F}{F_{th}}\right) \quad (1)$$

where, d(F) represents the ablation rate per pulse and α_{eff} is the effective absorption coefficient. F_{th} is defined as the minimum fluence at which the onset of ablation can be observed.

3. Results and discussions

3.1. Characterization

Starting from the information obtained on the polyacrylates studied earlier [20], where the nature of substituent attached to the triazene chromophore is one of the main factors that can modulate the photosensitivity of polymers; we extended this study on new triazene polyacrylates prepared through free-radical

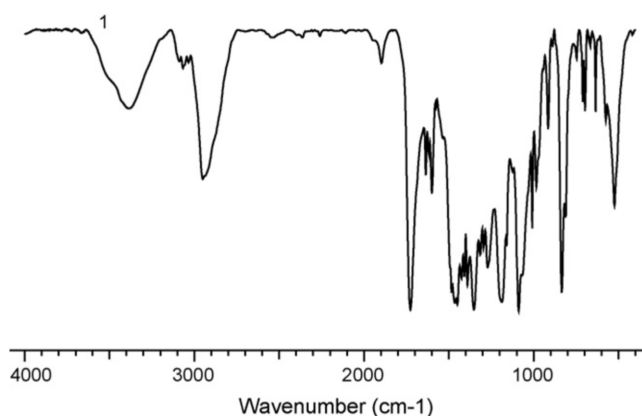

Fig. 1. Infrared spectrum of M_2.

polymerization between the triazene monomers and methyl methacrylate (MMA). Therefore, two new triazene monomers (M_1 and M_2) were synthesized by N–N coupling of the aromatic diazonium salt with *N*-methylaminoethanol followed by esterification of the formed intermediates (I_1 or I_2) with acryloyl chloride, according to Scheme 1. The structure and purity of the synthesized products was confirmed by FTIR, ^{1}H NMR and UV spectroscopy, as well as by elemental analysis.

Infrared analysis provides information about the molecular structure of the compounds. For example, the FT-IR spectrum of the second monomer (M_2) (Fig. 1) shows some characteristic bands at 1635 cm^{-1} (C=C) and 1352 cm^{-1} recognized for triazene units. The stretching vibration of the aromatic ring appears at 1599 cm^{-1} and 834 cm^{-1}(disubstituted aromatic ring), while the broad peak around 1720 cm^{-1} is assigned to the carbonyl group. The first monomer has an IR spectrum analogous to that of M_2, excepting the band at 1190 cm^{-1}, where is identified the vibration of OCH_3 group.

The ^{1}H NMR spectrum of (1-(*para* chloro-phenyl)-3-(2 acryloyloxyethyl)-3-methyl triazene-1, M_2) given in Fig. 2, was in accord with the expected structure. The singlet peak at around 7.42 ppm is attributed to the aromatic protons, whereas the protons from *ortho* and *meta* position to triazene groups of M_1 appear as two doublets at 7.34 ppm and 6.83 ppm, respectively (see Section 2.2). This later detail is caused of the electronic effects of methoxy substituent in *para* position. Proton peaks at 6.15 ppm (*trans* olefinic proton CH_2), 6.13 ppm (olefinic proton CH) and 5.8 ppm (*cis* olefinic proton CH_2) are detected besides the peaks of the ethylene protons from ester group that become visible at 4.4 ppm (CH_2CH_2OCO) and 4.05 ppm

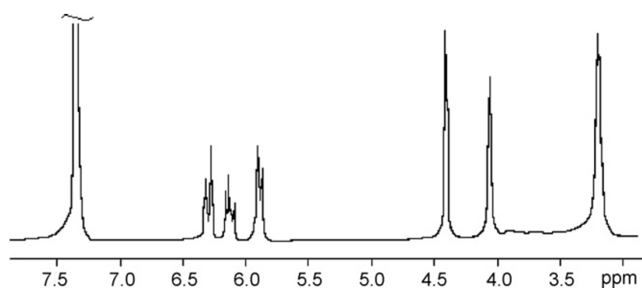

Fig. 2. ^{1}H NMR spectrum of M_2.

Table 1
Thermal behavior of triazene copolyacrylates

Sample	Stage I			Stage II		
	$T_i - T_f$ (°C)	T_{max}	Weight loss (%)	$T_i - T_f$ (°C)	T_{max}	Weight loss (%)
PA1	78–146	138	10	146–417	350	80
PA2	125–265	200	15	265–450	370	80

(CH_2CH_2OCO). The peak at around 3.20 ppm is assigned to methyl protons of the triazene group.

As shown in Scheme 2, the corresponding copolymers (PA1 and PA2) were prepared by free-radical polymerization of M_1 or M_2 with MMA (70% conversion) using AIBN as the initiator. Both polymers present a high solubility in common solvents such as DMF, DMSO, chloroform, and dichloromethane, and have good film-forming properties.

In the IR spectra, the acrylic copolymers display absorption bands of the starting monomers, not including the stretching vibration of the C=C double bond, which confirms that the polymerization of monomeric units occurred. Characteristic of the triazene structure chemically anchored to the polymeric chain is the absorption at 1375 cm^{-1}.

The copolymer composition was calculated from the relative intensities of the aromatic protons from M_1 (7.3–6.9 ppm) and the aliphatic protons signals of CH_3, CH_2 and CH (2.1–1.4 ppm) from monomers. The molar fraction of M_1 in the PA1 copolymer is 0.16. Similarly, it was also determined the copolymer composition in the case of PA2 (the molar fraction of $M_2 = 0.11$). The content of triazene units in the obtained copolymers was smaller than that of the monomer feed ratio (1:2.33), due to the more frequent attack of the MMA radical to itself monomer. This observation is quite close from that found for a copolyacrylate based on MMA and ethylacrylate, known for its different reactivity [23].

The weight-average molecular weights (Mw) of the triazene polymers determined by GPC with respect to monodisperse polystyrene standards indicated values of 85,000 for PA1 and 108,000 for PA2, with a polydispersity (Mw/Mn) of 1.8 for PA1 and 1.85 for PA2, respectively.

Thermal behavior of PA1 and PA2 was studied by thermogravimetric (TGA) and differential scanning calorimetry (DSC) analysis. The results of thermal stability showed in Table 1, indicates a two-step decomposition process that started relatively early, the initial decomposition temperature for PA1 and PA2 being remarked below 150 °C. In the second step, the process continues with the complete degradation of the macromolecular chains of triazene photopolymers (Fig. 3). The literature data suggests that polymers with a big amount of photolabile chromophore like triazene units have a poor thermal stability [24], at this point we should note that in our case, the weight loss observed in the first stage of the process can be attributed to the triazene group decomposition with releasing of small volatile molecules, such as molecular nitrogen and aromatic compounds. DSC thermograms of the two runs performed for both copolymers exhibit a single broad endotherm that is usually associated with the glass transition temperature for each triazene polyacrylate (Fig. 4). Moreover, the presence of one T_g indicates that the copolymer was miscible according to the composition obtained in this work. PA1 shows a T_g value of 45 °C, which is lower than that of PA2 at 62 °C and this effect is a consequence of increasing flexibility in the former.

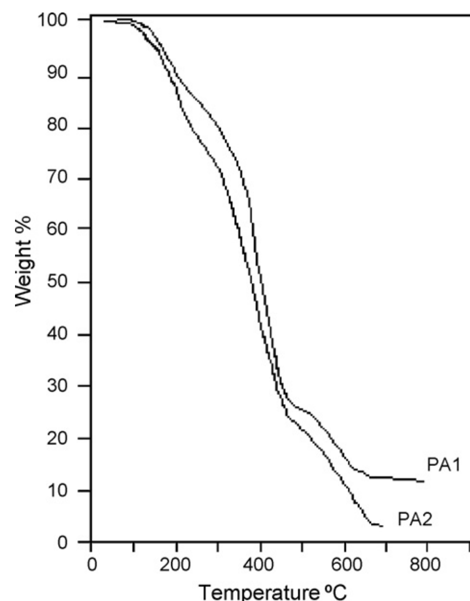

Fig. 3. TGA thermograms of the triazene copolyacrylates.

3.2. Photobehavior studies

As already reported [15], the choice of triazene chromophore is mainly motivated by the possibility to correlate its absorption maximum in the UV spectrum with laser radiation wavelength. Because one of the most profitable ways is attaching of appropriate substituents in the vicinity of the triazene group from

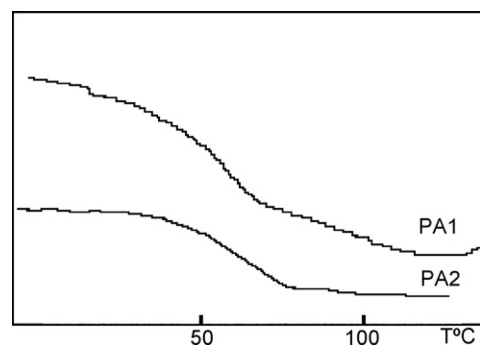

Fig. 4. DSC traces for both triazene copolymers.

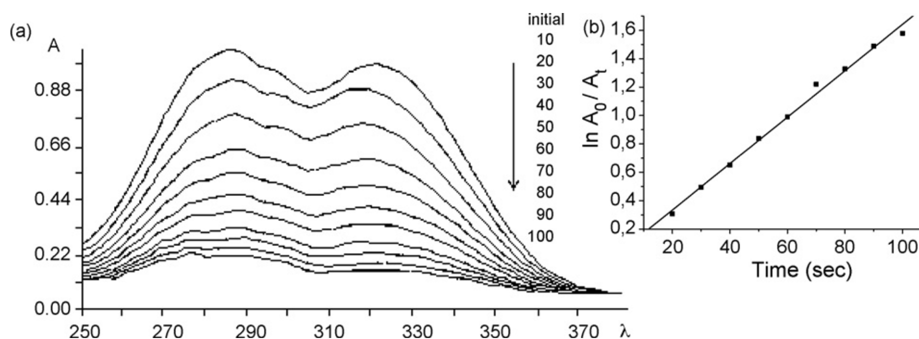

Fig. 5. UV–vis spectrum of *para*-methoxy intermediate (I_1) in methanol solution (a) and its kinetic evaluation (b).

the polymer backbone, we began through examining the photodecomposition of the triazene moiety both in the triazene intermediates and the corresponding copolymers. Decrease in the chromophore concentration with irradiation time was monitored firstly in solution, through irradiation with a high-pressure mercury lamp. In our case, the triazene chromophore presents in the UV spectra two broad absorption maximum attributed to π–π^* transitions, centered at 290 nm and 325 nm for I_1 (Fig. 5(a)), while the I_2 has the absorption peaks at 288 nm and 320 nm, respectively.

Under UV irradiation, the triazene group is decomposed with the release of molecular nitrogen and aromatic compounds—a process that is reflected in the UV spectra by a gradual decreasing of the absorption maximum up to a limit, when it is supposed that the most triazene units are decomposed, and UV absorption tends to zero. For I_1 the photodecomposition was almost completed within about 1.6 min (95%), a time period shorter than in the case of *para*-chloro triazene intermediate (I_2), where the same process took place in about 41 min (not shown here). Such spectral changes are reflected in the photolysis rate values, for which the rate constant k was determined according to equation:

$$\ln \frac{A_0}{A_t} = kt$$

where, A_0 and A_t are the values of the absorbance at times t_0 and t, respectively, and k is a rate constant. Accordingly, the k value calculated for I_1 is $k = 1.60 \times 10^{-2}\ \mathrm{s}^{-1}$ comparing with I_2, where the conversion is lower ($k = 6.70 \times 10^{-4}\ \mathrm{s}^{-1}$). The kinetic representation obtained by plotting the logarithm of the reduced absorption against time indicates a first-order kinetic of the photo process (Fig. 5(b)).

To obtain more information about the substituent effects, we have investigated the structural changes of the triazene chromophore in each copolymer. For the PA1 solution, the absorption maxima are centered at 290 nm and 330 nm. In Fig. 6(a) a typical example for the change of UV absorption curve during photodecomposition, where the triazene chromophore absorption band flattens first and then continues to decrease with irradiation time indicating a degree of polymer photodecomposition of about 50% (4.5 min) is presented. A comparison of the kinetic plots indicates that this reaction took place faster for PA1 ($k = 2.80 \times 10^{-3}\ \mathrm{s}^{-1}$) in a DMF solution (Fig. 6(b)) than for PA2 ($k = 4.0 \times 10^{-4}\ \mathrm{s}^{-1}$). Moreover, for both polymers, the photo process follows first-order kinetics that illustrate rather differences between rate constants, probably due to the electronic effects of the two substituents (Cl, OCH_3) of the triazene chromophore. All these experiments were done to prove again [20,21] that the photosensitivity of the triazene moiety strictly depends on the conjugation effects generated by the nature of substituents in the chromophore neighborhood. As a consequence, *p*-chloro electron-withdrawing substituent increased the stability of polymers at UV photolysis.

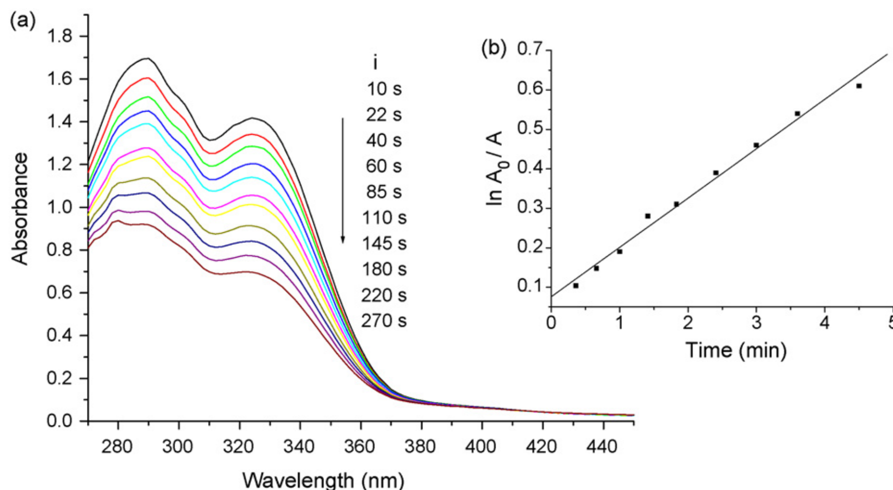

Fig. 6. Changes in the UV spectra of *p*-methoxy copolymer (PA1) in DMF solution with irradiation time (a) and kinetic evaluation of the photolysis (b).

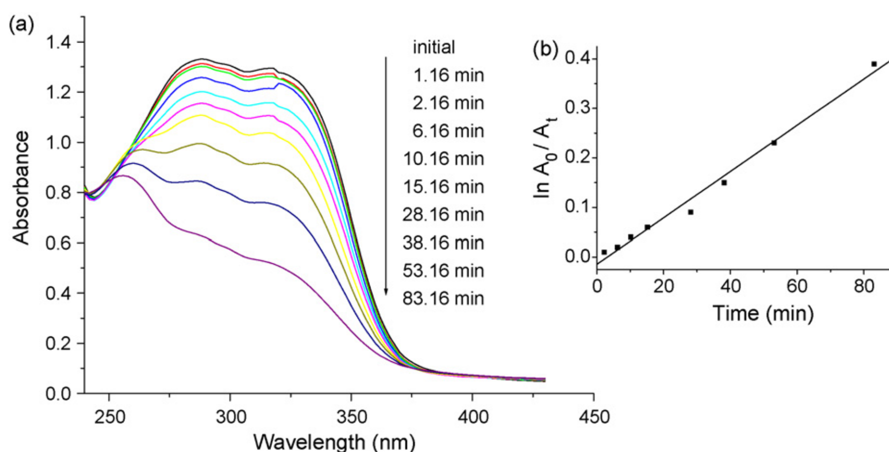

Fig. 7. Initial UV absorption curve and photodecomposition of *p*-chloro triazene polymer (PA2) in film state (a) and the first-order kinetic estimation of the photolysis (b).

To analyze the photochemical behavior of the triazene polyacrylates intended for photolithographic materials, polymeric thin films were irradiated with UV light under the same experimental conditions. Thus, the photolytic degradation of the PA1 film proceed in 15 min with a rate constant of $k = 2.3 \times 10^{-3}\ s^{-1}$, whereas for PA2 film the photodecomposition of the triazene unit took place in 80 min, the rate constant being $k = 2.7 \times 10^{-4}\ s^{-1}$ (Fig. 7). Comparing the results obtained in the case of triazene polymers discussed above, it is seen that photosensitivity of the triazene moiety to UV irradiation in polymer solution slightly increased. A logical explanation can be given by the faster decomposition of the triazene-containing polymer at 308 nm in solution, where thermal considerations are less important.

3.3. Atomic force microscopy (AFM) images

The surface topography of the triazene copolyacrylates has been visualized with AFM. The polymeric films for AFM experiments were prepared by solvent casting from a 2% DMF solution on a quartz substrate. For checking the reproducibility of the pictures and for a better visibility of the details, the images were registered in different points of the substrate with a scanning area of 5 μm × 5 μm or 10 μm × 10 μm. Fig. 8 shows a schematic representation of the surface morphology in thin film suggesting a homogeneous structure of the polymers [25]. These micrographs evidence the presence of a nearly smooth surface with little height differentiations and a relatively uniform topographical pattern. Although PA1 and PA2 form a good-quality film, these differentiations regarding the height lead to a surface roughness including hills and valleys with an average height of 50 nm for PA1 and respectively, 6 nm for PA2. The height and diameter characteristics have been confirmed by a cross section of the film. This segment seems to confirm the presence of nanophase-separated domains and small aggregates of various sizes distributed over the entire surface, as indicated the profilometric curve attached to Fig. 8.

3.4. Laser ablation

In addition to UV investigations, the triazene copolyacrylates PA1 and PA2 were subjected to laser irradiation in order to evaluate the influence of laser beam on polymer surface. Generally, photopolymers exhibit high photosensitivity and this concept was used to test if the incorporation of photochemically active groups on the polymeric chain improves the ablation characteristics. For an application standpoint, the polymeric films were

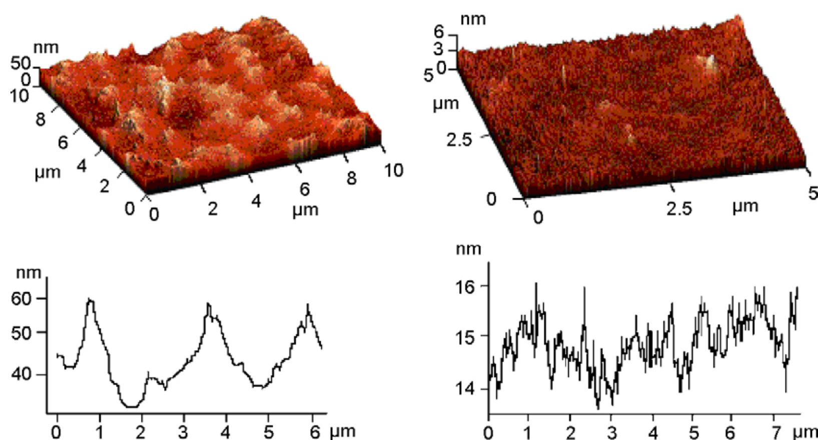

Fig. 8. 3D and section analysis AFM images obtained for PA1 (a) and PA2 (b).

Table 2
Ablation parameters of triazene copolyacrylates

Sample	F_{th} (mJ cm^{-2})	α_{eff} (cm^{-1})	α_{lin} (nm)
PA1	211	5743	12.000
PA2	112	10,593	32.000
Other triazene-containing polymers [20]	60–70	11,000–35,000	31,000–52,000

prepared by spin-coating a cyclohexanone solution on a quartz plate, and then irradiated with a XeCl excimer laser (308 nm). The polymers were studied at low fluences (between 10 mJ cm^{-2} and 400 mJ cm^{-2}), where the influence of structural parameters on the ablation rate can be observed. The ablation parameters, F_{th} (threshold fluence) and α_{eff} (effective absorption coefficient) calculated according to the Eq. (1), indicate that *p*-methoxy triazene copolymer PA1 has a threshold fluence of 211 mJ cm^{-2}, while for the second copolymer with *p*-chloro substituent in the backbone, F_{th} is much lower (F_{th} = 112 mJ cm^{-2}) (Table 2). Viewed from the economic perspective, a polymer with a threshold fluence as low as possible is desired. The lower F_{th} value in the case of PA2 clear sustains that the *p*-chloro substituent is less sensitive to 308 nm irradiation than the methoxy triazene group (PA1), due to electron-withdrawing character of the former that increased the stability of polymers exposed to UV photolysis. For that reason, the high stability of the PA2 to UV irradiation could be encouraging for laser structuring applications where no modification of the polymer under ambient conditions is preferred. Therefore, it becomes clear in Table 2 that the introduction of Cl, OCH_3 or NO_2 substituents in phenyltriazene acrylates [20] had a pronounced influence on the ablation characteristics (F_{th}, α_{eff}) of the resulting copolymers, a good ablation behavior being observed in the case of polymer containing non-substituted triazene.

On the other hand, the effective absorption coefficient of ablation is 5743 cm^{-1} for PA1 and 10,593 cm^{-1} for PA2, respectively. The higher α_{eff} value corresponds to high ablation rates for PA2, and α_{eff} decreases with increasing fluence as shown in Fig. 9, where the ablation rate is plotted against the irradiation fluence.

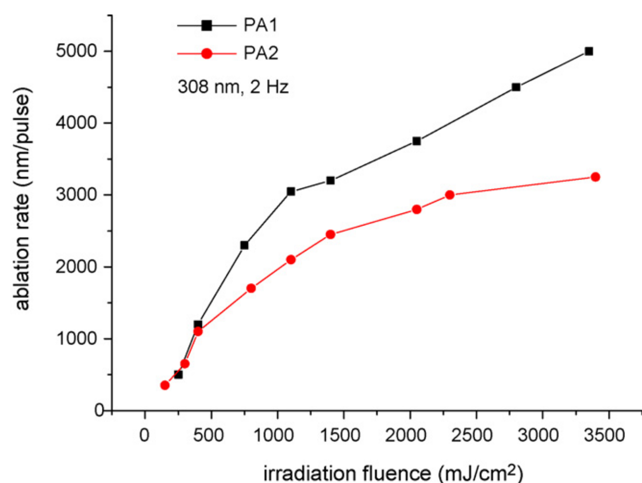

Fig. 9. Ablation rate as a function of the laser fluence for 308 nm irradiation of the triazene polymers PA1 and PA2.

The effective absorption coefficients do not correlate with the linear absorption coefficients (Table 2). Both polymers, in this study, can be classified as highly absorbing polymers (α_{lin} larger than 8000 cm^{-1} at the irradiation wavelength of 308 nm). In addition, the measured α_{lin} of the copolyacrylates are higher than the values of the α_{eff} calculated from the aforementioned relation. An explanation of these differences can be the broken of the N–N bond by the XeCl excimer laser (308 nm = 4.02 eV) during the laser ablation process [26].

The morphology of the polymeric films after laser ablation was illustrated by optical microscopy. In Fig. 10, the photographs of the PA1 (a) and PA2 (b) structures are shown as examples. Both the ablation spots were made after 10 pulses at 70 mJ cm^{-2}, 140 mJ cm^{-2} and 420 mJ cm^{-2} fluence. It can be remarked straight, sharp and no damage limits with flat and smooth bottoms, indicating no pronounced thermal degradation. Moreover, the ablation of the triazene polyacrylates is dominated by the absence of debris in the areas surrounding the craters, whereas in the dark area around the ablated surface is the unmodified polymer. These photoimages confirm a well-defined structuring of the investigated polymers due to the decomposition of triazene moieties, for which a clean surface is very important for its application in lithography. As anticipated, from the size of the microridges, the resolution is, in the micrometer or even submicrometer domain; where the absorption of the photo-

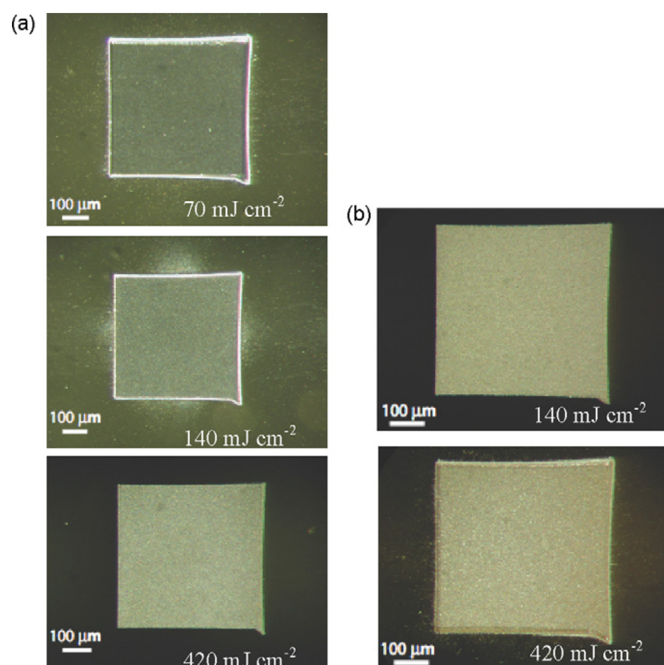

Fig. 10. Optical micrographs of the ablated craters (308 nm) for PA1 (a) and PA2 (b) after 10 pulses at different fluences.

chemically active groups can be decoupled with the absorption of the other parts of the polymer structure.

However, the experimental results show that the designed polymers are ablated without major modifications of the surface, thus allowing a reproducible ablation. Such polymers seem to be rather suitable for applications in the fast fabrication of microstructures with enough precision by using excimer laser ablation at 308 nm.

4. Conclusions

Two new acrylic monomers with triazene moieties incorporated on the polymeric backbone were synthesized and characterized. Further reactions, between acrylic monomers and MMA lead to photopolymers with triazene units on the backbone, which can be used for UV/laser photolithography. The photosensitivity was detected by irradiating and monitoring the behavior of copolymers through UV spectroscopy. The copolymer with the *para*-chloro triazene moieties is more stable under UV irradiation compared to that containing *para*-methoxy unit and displays superior properties for UV/laser applications. The experiments performed with the excimer laser irradiation (308 nm) demonstrated that the designed copolymers could be used for the fabrication of microstructures. Therefore, the generated microridges illustrate the absence of any amount of red posited material and achieving of a flat and smooth surface.

Acknowledgment

The authors would like to thank the Ministry of Research and Education for the financial support of this work by a project from The National Plan of Research & Development- PNII (IDEI Program: project no. 78/1.10.2007).

References

[1] K. Morigaki, H. Schönherr, C.W. Frank, W. Knoll, Langmuir 19 (2003) 6994.
[2] C.A. Rouzer, M. Sabourin, T.L. Skinner, E.J. Thompson, T.O. Wood, G.N. Chmurny, J.R. Klose, J.M. Roman, R.H. Smith, C.J. Michejda, Chem. Res. Toxicol. 9 (1996) 172.
[3] A. Natansohn, P. Rochon, Chem. Rev. 102 (2002) 4139.
[4] B. Sieczkowska, M. Millaruelo, M. Messerschmidt, B. Voit, Macromolecules 40 (2007) 2361.
[5] D.B. Kimball, M.M. Haley, Angew. Chem. Int. Ed. 41 (2002) 3338.
[6] P. Gupta, S.R. Trenor, T.E. Long, G.L. Wilkes, Macromolecules 37 (2004) 9211.
[7] O. Nuyken, U. Dahn, Chem. Mater. 9 (1997) 485.
[8] K. Suzuki, M. Matsuda, T. Ogino, N. Terabayashi, K. Amemiya, Proc. SPIE 2992 (1997) 98.
[9] T. Lippert, J. Wei, A. Wokaun, N. Hoogen, O. Nuyken, Appl. Surf. Sci. 168 (2000) 270.
[10] Z. Chen, D.C. Webster, J. Photochem. Photobiol. A: Chem. 185 (2007) 115.
[11] T. Lippert, A. Yabe, A. Wokaun, Adv. Mater. 9 (1997) 105.
[12] Ch. Hahn, T. Lippert, A. Wokaun, J. Phys. Chem. B 103 (1999) 1287.
[13] T. Lippert, Plasma Process. Polym. 2 (2005) 525.
[14] T. Lippert, Adv. Polym. Sci. 168 (2004) 51.
[15] T. Lippert, J.T. Dickinson, Chem. Rev. 103 (2003) 453.
[16] F. Raimondi, S. Abolhassani, R. Brütsch, F. Geiger, T. Lippert, J. Wambach, J. Wei, A. Wokaun, J. Appl. Phys. 88 (2000) 3659.
[17] R. Fardel, M. Nagel, F. Nüesch, T. Lippert, A. Wokaun, Appl. Phys. Lett. 91 (2007) 061103.
[18] J. Xu, J. Liu, D. Cui, M. Gerhold, A.Y. Wang, M. Nagel, T. Lippert, Nanotechnology 18 (2007) 025403.
[19] A. Doraiswamy, R. Narayan, T. Lippert, L. Urech, A. Wokaun, M. Nagel, B. Hopp, M. Dinescu, R. Modi, R. Auyeung, D. Chrisey, Appl. Surf. Sci. 252 (2006) 4743.
[20] E.C. Buruiana, T. Buruiana, L. Hahui, T. Lippert, L. Urech, A. Wokaun, J. Polym. Sci. Part A: Polym. Chem. 44 (2006) 5271.
[21] E.C. Buruiana, V. Melinte, T. Buruiana, T. Lippert, H. Yoshikawa, H. Mashuhara, J. Photochem. Photobiol. A: Chem. 171 (2005) 261.
[22] J.E. Andrews, P.E. Dyer, D. Forster, P.H. Key, Appl. Phys. Lett. 43 (1983) 717.
[23] J.C. Bevington, D.O. Harris, J. Polym. Sci. B 5 (1967) 799.
[24] N. Hoogen, O. Nuyken, J. Polym. Sci. Part A: Polym. Chem. 38 (2000) 1903.
[25] E.C. Buruiana, V. Melinte, T. Buruiana, B.C. Simionescu, T. Lippert, L. Urech, J. Photochem. Photobiol. A: Chem. 186 (2007) 270.
[26] J. Wei, T. Lippert, N. Hoogen, O. Nuyken, A. Wokaun, J. Phys. Chem. B 105 (2001) 1267.